JOURNAL OF OCULAR PHARMACOLOGY AND THERAPEUTICS
Volume 23, Number 4, 2007

DOI: 10.1089/jop.2006.0135

Zinc Phthalocyanine Tetrasulfonate ($ZnPcS_4$): A New Photosensitizer for Photodynamic Therapy in Choroidal Neovascularization

YAN HUANG,[1,2] GUOXING XU,[1,2] YIRU PENG,[3] HONG LIN,[1] XUEDONG ZHENG,[1] and MAOSONG XIE[1]

ABSTRACT

Purpose: **The aim of this sutdy was to demonstrate the selective localization of a new photosensitizer, zinc phthalocyanine tetrasulfonate ($ZnPcS_4$), in rat eyes and investigate the ability of $ZnPcS_4$ to produce a photochemical closure of experimental choroidal neovascularization (CNV) upon irradiation with a 670-nm laser light.**

Methods: **To determine the biodistribution of $ZnPcS_4$ and the optimal timing of laser irradiation after photosensitizer administration, fluorescence microscopy with $ZnPcS_4$ was performed. CNV was created in the fundi of Brown-Norway rats using the argon laser model and documented by fluorescein angiography (FFA) and optical coherence tomography (OCT). Photodynamic therapy (PDT) was performed at the dose of 2.0 mg/m^2 and laser fluences of 600 mW/cm^2 on the CNV and on normal retina and choroid. Treatment outcomes were assessed by FFA and OCT and confirmed by light and electron microscopy.**

Results: **Fluorescence microscopy demonstrated intense $ZnPcS_4$ fluorescence from the CNV, choriocapillaris, and retinal pigment epithelial cells. Peak $ZnPcS_4$ intensities in the choriocapillaris and CNV were detected at 10–20 min after an intravenous injection. FFA and OCT indicated that irradiation with 670 nm of laser light 20 min after a $ZnPcS_4$ injection produced a complete closure of CNV with minimal damage to the overlying retina. Histologic studies, using light and electron microscopy, demonstrated CNV endothelial cell necrosis with minimal damage to the surrounding tissues.**

Conclusions: **$ZnPcS_4$ selectively localizes to the choriocapillaris and CNV in rats, resulting in the occlusion of laser-induced CNV with minimal damage to the retina tissues. $ZnPcS_4$–PDT is a potential new strategy for the treatment of macular degeneration and other human diseases manifesting as CNV.**

INTRODUCTION

Age-related macular degeneration (AMD) is the leading cause of severe vision loss in people older than 65 years of age in most countries. Eighty percent (80%) of exudative AMD in patients with severe vision loss is the result of choroidal neovascularization (CNV).[1] Recently, there has been much interest in photodynamic therapy (PDT) for AMD. PDT is a technique that

[1]Department of Basic Medical Science, the Affiliated First Hospital of Fujian Medical University, Fujian, China.
[2]Department of Ophthalmology, Shandong University, Fuzhou, China.
[3]College of Chemistry & Materials, Fujian Normal University, Fujian, China.

uses light-activated drugs and nonthermal light to achieve the selective, photochemical destruction of diseased cells with minimal effect on the surrounding normal tissues.[2,3]

The mechanism of PDT is postulated to involve the release of excited oxygen species that activate the subendothelial clotting cascade and result in the selective occlusion of the CNV.[4,5] Because photosensitizers can be administered intravenously (i.v.) and have been demonstrated to accumulate in CNV membranes, they might preferentially occlude CNV with diminished damage to collateral structures, such as the retinal pigment epithelium (RPE) and inner retina. This selective occlusion is enhanced by the apparent affinity of the various photodynamic agents for CNV, with relative sparing of the retina and its vessels. Verteporfin (Visudyne; Novartis AG, Basel, Switzerland), the only approved photosensitizing agent currently available for ophthalmic indications, shows a limited benefit and is associated with the recurrence of the CNV associated with AMD, requiring three retreatments over the first year.[6] Notably, Verteporfin is too expensive for most patients to afford. Consequently, there is much interest in developing new photosensitizing agents with better efficacy and selectivity. Some of the photosensitizers currently being developed in animal models include lutetium-texaphyrin,[7] chlorin e6,[8] tin ethyl etiopurpurin,[9] ATX-S10 (Na),[10] and PhotoPoint photosensitiser MV6401.[11] Numerous photodynamic agents in various phases of development have also been described.

The new photosensitizer, phthalocyanine zinc, has also recently shown efficacy in the treatment of CNV in experimental models.[12,13] The phthalocyanine group includes zinc phthalocyanine disulphonate, chloroaluminum phthalocyanine tetrasulfonate, zinc phthalocyanine tetrasulfonate ($ZnPcS_4$), and aluminum phthalocyanine tetrasulfonate ($AlPcS_4$). Phthalocyanines have distinct advantages over other photosensitizers: They are easily prepared as chemically pure compounds,[14] offer hydrophilic solution preparation (which allows for i.v. bolusing), have both high affinity for neovascular tissues and high photosensitizing ability as well as rapid tissue uptake and clearance, have minimal systemic toxicity, and cause minimal skin photosensitization.[15] Most important, they have a long wavelength absorption peak (670 nm), which potentially allows for a greater penetration of exciting light through tissues, pigment, fluid, and blood. Previous authors have studied the photodynamic effects of sulphonated zinc and aluminum phthalocyanine derivatives, as well as phosphonated aluminum phthalocyanine, on the firing of isolated crayfish mechanoreceptor neurons. Kliman and colleagues[12] have proposed that chloroaluminum sulfonated phthalocyanine (CASPc), a photochemically active dye employed in photodynamic therapy (PDT), localizes in neovascular choroidal vessels and that CASPc photodynamic therapy can produce a closure of these choroidal vessels. Peèkaitytëa and coworkers[16] have shown that the phototoxic activity of photosensitisers against all bacterial strains tested increases in the order of $AlPcS_4 < ZnPcS_4$. $ZnPcS_4$ is a promising second-generation photosensitizer for use in medicine, but it cannot be applied clinically until safety and efficacy data are available. Based on these data, a phase I clinical trial of $ZnPcS_4$-based PDT in tumor-bearing dogs is underway, with $ZnPcS_4$ doses up to 2 mg/m^2 producing no apparent toxicity.[17] However, to the best of our knowledge, this is the first application of $ZnPcS_4$–PDT in the rat CNV model.

The aim of this study was to determine the selective localization of the new photosensitizer $ZnPcS_4$ in the choriocapillaris and CNV in rat eyes, and to then investigate the ability of $ZnPcS_4$ to produce photochemical closure of neovascularization upon irradiation with 670 nm of laser light. The nature of the histologic changes in the choroid, CNV, RPE, and retinal vessels following $ZnPcS_4$–PDT were observed.

METHODS

Photosensitizer

$ZnPcS_4$ was provided by the College of Chemistry & Materials of Fujian Normal University (Fujian, China). Its purity was >98%, and its chemical structure is shown in Figure 1. The agent was stored at 2–8°C. The vials were wrapped in aluminum foil to avoid light exposure at all times. Immediately before injection, the dyes were dissolved in Dulbecco's phosphate-buffered saline (DPBS) to a concentration of 1.0–2.0 mg/mL. The solutions were passed through a 0.22-μm filter before injection.

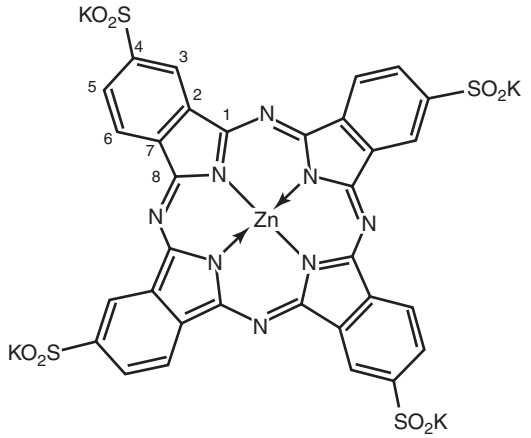

FIG. 1. The structure of $ZnPcS_4$.

Laser delivery system

A diode laser (LD-670; Tianjin Medical University, Tianjin, China) emitting at a wavelength of 670 nm and mounted on a modified Topcon slit-lamp adaptor (Laserlink; Coherent Medical Laser, Santa Clara, CA) was employed for PDT experiments.

Animals

All experiments were conducted in accordance with the resolutions on the use of animals in research developed by the Association for Research in Vision and Ophthalmology and the guidelines developed by the Indiana University Animal Care and Use Committee (Bloomington, IN). Fifty-six (56) Brown-Norway rats (112 eyes), weighing between 0.25 and 0.30 kg, were studied. Before all experiments, the animals underwent an initial baseline examination to rule out preexisting pathology and to document the baseline condition of the subjects assigned to the study. Clinical examinations were conducted by slit-lamp biomicroscopy, indirect ophthalmoscopy, or fundus photography. All rats were divided into two groups at random: 20 rats underwent fluorescence microscopy and 36 rats PDT. For all procedures, the rats were anesthetized with 0.1–0.2 mL of a 50:50 mixture of 100 mg/mL of ketamine and 20 mg/mL of xylazine. Topical tropicamide (0.8%) and phenylephrine hydrochloride (2.5%) were administered for pupillary dilation and cycloplegia. Before enucleation, animals were sacrificed under deep anesthesia with pentobarbital sodium (i.v., 50 mg/mL) injection.

CNV model

Thirty-six (36) rats and 36 eyes were used for photocoagulation. Three spots were created in every eye. Photocoagulation burns were created on the fundus, using a 532-nm Laser from Zeiss (Carl Zeiss; Jena, Germany), with the following parameters: a 532-nm wavelength, 100-μm spot size, 0.1-s duration, and 800 mW of power.[12] The endpoint of photocoagulation was the observation of optical bubbles, subretinal hemorrhage, or retinochoroidal whitening.

FFA and OCT

On day 1 and weekly for 4 weeks after photocoagulation, an ophthalmoscopic examination, fundus fluorescein angiography (FFA), and optical coherence tomography (OCT) were performed to document the presence of CNV. Baseline FFA was performed by using 25% sodium fluorescein (0.1 mL/kg) administered through the tail vein. Fundus photographs of selected areas on the retina were taken during this baseline examination by using a modified Canon fundus camera (CF60UV; Canon Co., Tokyo, Japan).

In our study, we used the Zeiss Optical Coherence Tomographer Model 3000 OCT3; Zeiss, Carl Zeiss). Pupils were dilated. Internal fixation, guided by the video image, was used to ensure that scans passed through the light spot or within two papilla diameters from the optic disc, as determined on the screen of the SLO (San Luis Obispo) monitor. We also obtained horizontal single-line scans of default length 4 mm at 0 degrees through the spot and a fast retina thickness map consisting of six simultaneous 3-mm radial-line scans. The centers of the photocoagulated lesions, including the surrounded normal tissues, were scanned by OCT.

Fluorescence microscopy

Ten (10) normal rats and 10 rats with CNV were used for fluorescence microscopy. Two (2) normal and 2 CNV eyes were enucleated at each time point of 5, 10, 20, 30, and 60 min after an $ZnPcS_4$ injection at a dose of 1.0 or 2.0 mg/m^2. Enucleation was performed with the animals under deep anesthesia and the eyeballs were sectioned, embedded in optimal cutting temperature solution (Sigma), and frozen at -70°F. Fifteen (15) unstained frozen sections were prepared with the use of a cryostat in subdued light. Pictures of

green fluorescence were taken with a Leica DMLB microscope (Leica Microsysteme Vertrieb, Bensheim, Germany). The filter sets that were used included an excitation bandpass filter, a dichroic beam splitter filter with 50% transmission-reflection, and an emission bandpass filter. The bandpass filters were centered at 300–500 nm (excitation) and 670 nm (emission). The fluorescence was observed as green light with these settings and recorded with color photomicrographs. Fluorescence was graded from nonfluorescent (0) to strongly fluorescent (++++).[18] The frozen sections were subsequently stained with hematoxylin and eosin (H&E) to facilitate the precise localization of the fluorescence.

Photodynamic therapy

PDT with $ZnPcS_4$ was performed on 12 rats with experimental CNV and 12 rats with experimental CNV laser irradiation, but without $ZnPcS_4$, 12 rats with experimental CNV were injected with $ZnPcS_4$ alone, without PDT. Anesthetized rats were immobilized on a stereotactic frame. PDT was performed 15 min after an injection of 2.0 mg/m^2 $ZnPcS_4$ into the tail vein. Six hundred and seventy (670) nm of laser light was administered with a diode laser that corresponded to the $ZnPcS_4$ photosensitizer, and was delivered through a slit-lamp adaptor. Laser power at the focal plane was measured with a power meter. The laser spot size was set at 800–1000 μm, and its size was confirmed with a micrometer. The laser spot size on the plane of the retina was the same as that at the plane of the cornea. The laser had a constant irradiance of 600 mW/cm^2 and was delivered for 80 s to achieve total energy doses of 50 J/cm^2.[15]

FFA and OCT were performed at 24 h and 7 days after PDT to evaluate CNV development and PDT results. CNV was defined as closed after treatment if there was an absence of leakage from the treated membrane, compared with baseline. All angiograms were evaluated in a masked manner by two experienced graders.

Histology

Eyes were enucleated on the same day after FFA and OCT. Enucleation was performed with animals under deep anesthesia, and the cornea and lens were removed. Each pair of eyes was immediately immersed in 10% formalin for 48 h after a choroid incision and then completely embedded in paraffin. The tissue was carefully trimmed to ensure that the tissue sample included the same retinal region as did the OCT images. Sections corresponding to the area of laser irradiation were stained with (H&E) to identify retinal structures. Further 5-μm-thick sections adjacent to selected areas were mounted on slides. The remaining tissue section was placed in a fixative containing 2.5% glutaraldehyde and 2% formaldehyde in 0.1 M of cacodylate buffer (pH, 7.4) at 4°C overnight. Tissue samples were postfixed in 2% osmium tetroxide, dehydrated in graded ethanol, and embedded in epoxy resin. For electron microscopic analysis, sections were stained with a saturated aqueous uranyl acetate solution and Sato lead stain (SPI (Structure Probe, Inc.) West Chester, PA). Sections were viewed with a transmission electron microscope (Hu-12A; Hitachi, Tokyo, Japan).

RESULTS

$ZnPcS_4$ fluorescence microscopy

The fluorescence of $ZnPcS_4$ at 1.0 mg/m^2 was below the resolution of our detection system. With the higher doses, 2.0 mg/m^2, we readily detected the fluorescence through the retinal and choroidal circulations. Scleral fluorescence was most prominent at 5 min. Choriocapillaris and CNV fluorescence was first detected at 10 min. At 20 min after an $ZnPcS_4$ injection, there was mild fluorescence in the choriocapillaris and maximal fluorescence was detected in the CNV. Inner retinal fluorescence was mild and somewhat increased at 10 min. The extent of fluorescence then diminished over the course of the study. Fluorescent imaging indicated that $ZnPcS_4$ was localized in areas of CNV for at least 30 min. No fluorescence could be detected at 60 min. As the mild fluorescence in the normal choriocapillaris and the maximal fluorescence in the CNV was detected at 20 min following the administration of the 2.0 mg/m^2 of $ZnPcS_4$ by the tail vein, we decided to administer the activating laser light for PDT during this time interval.

Representative fluorescence images that were obtained in the choriocapillaris and CNV are shown in Figure 2A–2C. The micrographs were

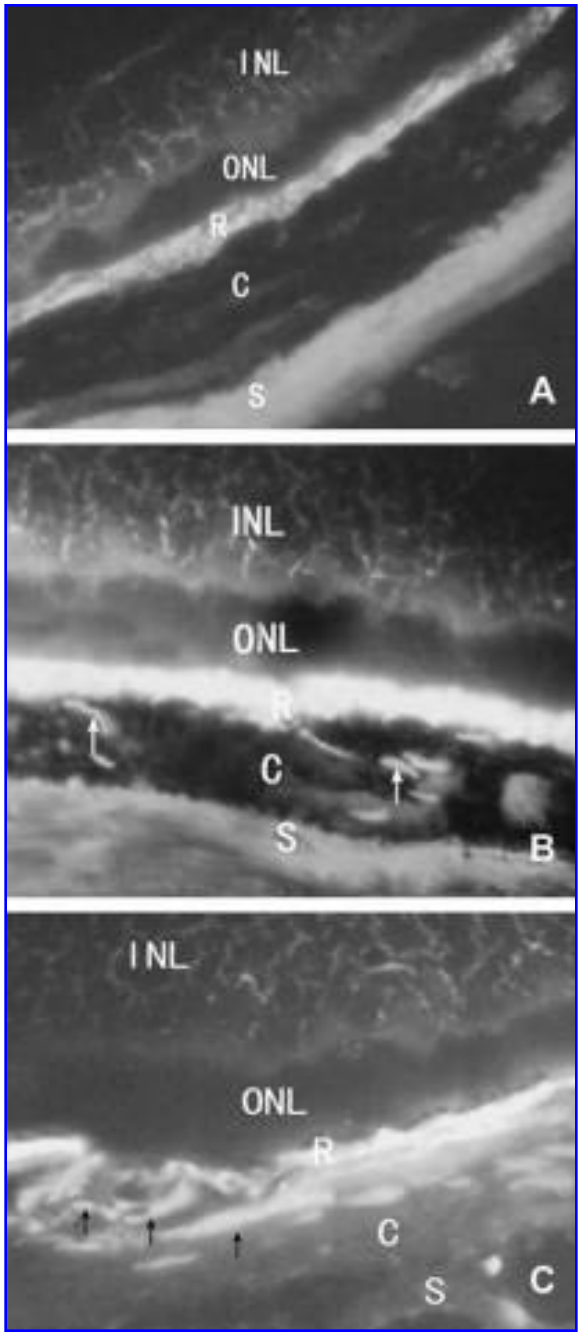

FIG. 2. Localization of $ZnPcS_4$ in rat eyes as detected by fluorescence microscopy. (**A**) In the retina of control group rats without a $ZnPcS_4$ injection, no fluorescence was detected. (**B**) At 10 min after a $ZnPcS_4$ injection, there was middle fluorescence in choriocapillaris (++) (white arrow) ¢Û At 20 min after a $ZnPcS_4$ injection, there was marked fluorescence in choroidal neovascularization (++++) (black arrow) The figures are intended to show the pattern of dye localization and are not intended to depict absolute intensity. INL, inner nuclear layer; ONL, outer nuclear layer; R, retinal pigment epithelium; C, choroid; S, sclera. Original magnification was ×200.

taken from the same region of the retina at the same magnifications.

Pre- and post-PDT fluorescein angiograms

An ophthalmoscopic examination of the fundus showed that the photocoagulated lesion appeared as a whitish-gray opacification of the retina (Fig. 3A). Three (3) weeks after photocoagulation, CNV was found in all rats, and FFA demonstrated hyperfluorescence of the experimental CNV, which increased in intensity in later frames (Fig. 3C and 3D). Immediately following treatment, fundus photography detected no obvious color change in the treatment zone. Seven (7) days following PDT, the treatment zone had developed a mild, deep-gray color change. One feature common to all lesions 24 h after PDT was the presence of a circle of choroidal hypofluorescence corresponding to the treatment zone. Lesions without PDT showed early hyperfluorescence in the center of the CNV treatment zone.

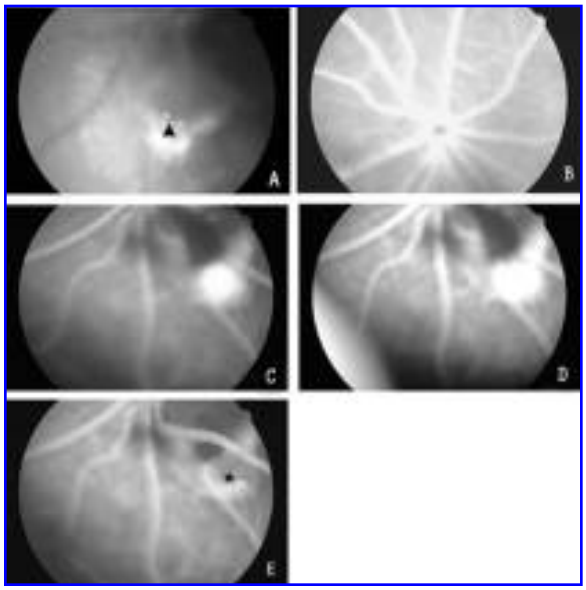

FIG. 3. Flourescein angiography taken pre- and post–photodynamic therapy (PDT) of rat eyes. (**A**) Fundus photography of rat retina 1 day after argon-laser photocoagulation. (**B**) Late phase of fluorescein angiogram of normal rat retina without fluorescein leakage. (**C**) Early phase of fluorescein angiogram of rat retina 3 weeks after argon-laser induction of choroidal neovascularization. Arrows: areas of fluorescein leakage at the site of the initial laser injury. (**D**) Late phase of the same fluorescein angiogram as shown in **C.** The two lesions with early hyperfluorescence showed a profuse leakage of fluorescein at 7 days after PDT. All late phase fluorescein angiogram lesions showed only some fluorescence, predominantly at the periphery of the treatment zone.

The hyperfluorescence then spread from the center of the CNV to encompass the whole treatment zone. The intensity of this fluorescence was often similar to that of untreated lesions. In contrast, lesions that responded to PDT did not show any early hyperfluorescence on FFA. Later in the course of the angiogram, there was typically some leakage of fluorescein into the treatment zone from the periphery of the zone of hypofluorescence (Fig. 3E).

Twenty-four (24) typical spots with CNV in 12 rats (two spots per rat in each group) were examined by FFA. The closure rates of the CNV 24 h and 7 days after PDT for the three groups are summarized in Table 1.

Pre- and post-PDT optical coherence tomography

OCT showed a double-layered structure in the normal sensory retina, with a highly reflective layer located in the inner retina and a minimally reflective layer located in the outer retina. The RPE and choriocapillaris were imaged as a layer with the highest red reflection. On the first day after photocoagulation, OCT showed a disruption of the highly reflective layer corresponding to the RPE, and an enhanced reflectivity in the choroid under the lesion. CNV, which appeared 3 weeks after photocoagulation, was seen as a nodular, highly reflective area protruding from the RPE into the subretinal space; no retinal detachment was found. An optical coherence tomogram of CNV taken 7 days after PDT revealed a white-colored highly reflective layer continuous with the RPE layer, with moderate reflection beneath the layer.

TABLE 1. CLOSURE RATE OF EXPERIMENTAL CHOROIDAL NEOVASCULARIZATION 24 H AND 7 DAYS AFTER PHOTODYNAMIC THERAPY (PDT)

Group	*Lesions closed at 24 h*	*Lesions closed at 7 days*
PDT	25 (6/24)	67 (16/24)
Laser irradiation alone	0 (0/24)	8 (2/24)
$ZnPcS_4$ alone without PDT	0 (0/24)	0 (0/24)

Note. The major difference was found between the 24-h and 7-day post-treatment closure rate. Animals receiving zinc phthalocyanine tetrasulfonate (ZnPcS4) alone without PDT or laser irradiation alone without $ZnPcS_4$ showed no sustained closure of the CNV, except at the 7-day post-treatment. The 24-h closure rate in these rats was 25% and increased to 67% at the 7-day post-treatment.

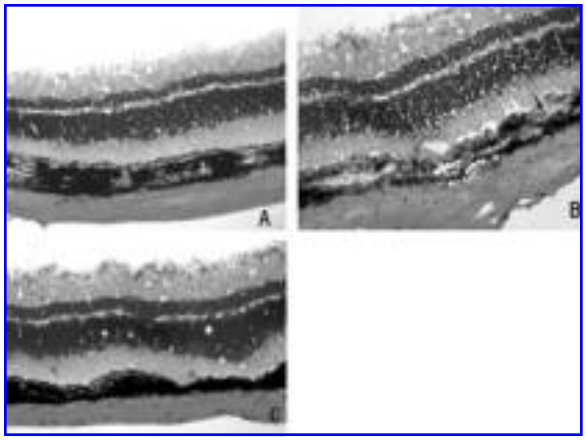

FIG. 4. Light micrographs (**A–C**) obtained before and 7 days after photodynamic therapy (PDT). (**A**) Histopathology of normal rat retina (HE, ×200). (**B**) Histopathology of a typical active choroidal neovascularization (CNV) (HE, ×200). Bruch's membrane is disrupted (black arrowhead), outer retina, choroid, and CNV. Note neovascular vessels filled with cellular debris (arrows) and proliferation of retinal pigment epithelium. Choriocapillaris that are adjacent to CNV have normal vascular lumens. In the inner retina, no obvious alteration is evident in the treated area. (**C**) Histopathology of a section of a CNV treated with $ZnPcS_4$ and fluence of 50 J/cm^2 at 7 days after PDT. This lesion was defined as closed, based on fluorescein angiographic analysis (HE, ×200).

Histopathologic features of $ZnPcS_4$ -PDT of CNV

A histopathology of normal rat retina is shown in Figure 4A. Figure 4B shows a light microscopic picture of untreated CNV 3 weeks after induction with the argon laser. A histopathology of a typical active CNV showed that the Bruch's membrane is disrupted and the surface of the membrane is enveloped by RPE cells. Macrophages with melanin granules are present in the outer layer of the retina, especially in the gap of the outer nuclear layer. There was a gross destruction of the outer retinal layers, RPE, and Bruch's membrane. Macrophages were seen in this zone of disrupted retina. Figure 4C shows a section of a CNV treated with 2.0 mg/m^2 of $ZnPcS_4$ and fluence of 50 J/cm^2 at 7 days after PDT. This lesion was defined as closed, based on FFA analysis. The surrounding retinal capillaries and choriocapillaris and the neurosensory retinal topographic architecture were intact.

Electron micrographs of normal rat retina is shown in Figure 5A; the nucleus of the RPE was clear, with a lot of pigment granules, a double layer of plasma membrane infolding above the

basement membrane line up in order, the Bruch's membrane is continuous in its integrity, and the wall of surrounding retinal capillaries and choriocapillaris were smooth with intact red blood cells in it. Laser-induced CNV in the rats showed morphologic features common to other models of CNV. Electron micrographs of the CNV demonstrated severe dysplasia of the endothelial cells and a loss of normal architecture, as evidenced by lumens filled with cytoplasmic debris and degenerated cellular blood components. There were vascular channels within a complex of fibrous proliferation, extending inwardly from the choroid through a gap in the Bruch's membrane (Figure 5B). $ZnPcS_4$ PDT caused a destruction of the vascular channels and an organization of the CNV complex into a scar with massive collagen fibers (Fig. 5C). The surrounding choriocapillaris (Fig. 5D) demonstrated no evidence of damage, but we observed some swelling and mitochondrial destruction in the RPE cells at the site of the PDT.

DISCUSSION

The stimulus for neovascularization in laser-induced lesion models obviously differs from that in AMD, as laser models invoke a traumatic repair process that may mimic traumatic CNV development better than AMD-related CNV. However, there are also substantial similarities between AMD-related CNV and laser-induced CNV. Dobi and colleagues[14] first proposed the rat model for laser-induced experimental CNV in 1989. Various aspects of CNV have been studied with this model. The laser used to induce the CNV created a disruption of the Bruch's membrane and RPE, two structures that are important in the functional separation of the choroid from the retina. Laser-induced CNV in the rats showed morphologic features common to other models of CNV. There were vascular channels within a complex of fibrous proliferation, extending inwardly from the choroid through a gap in the Bruch's membrane. David and colleagues[15] presented evidence that supports the use of experimental CNV treatment with verteporfin PDT in the rat as a valid and effective model of verteporfin PDT in humans. Verteporfin PDT is useful, but in humans its choroidal hypoperfusion causes notable damage and limits its use. Our study showed that the CNV rat model was developed 3 weeks after laser photocoagulation, and that this model can serve as a reasonable first step in the rapid analysis of potential therapies for CNV treatment and for assessing the effects of such therapies on both normal and abnormal structures, before proceeding to primate studies or to human clinical trials. Future trials will compare this treatment with verteporfin and will include post-treatment indocyanine green angiography to assess choroidal hypoperfusion.

This study evaluated the photosensitizer $ZnPcS_4$, an efficient generator of singlet oxygen, which shows peak absorption in the ultraviolet range and in red ranges between 670 and 680 nm. As noted previously, $ZnPcS_4$-based photodynamic therapy in ophthalmic applications has not been studied. In ophthalmic applications, it is activated by low-power, nonthermal laser light at 670 nm, which is thought to penetrate blood, melanin, and fibrous tissue. Rapid clearance of the photosensitizer from the normal circulation with selective retention in experimental CNV confers a hypothetical advantage over hydrophobic photosensitizers, both in terms of selectivity and of toxicity. The failure of $ZnPcS_4$ alone or laser irradiation alone to induce angiographic evidence of occlusion demonstrates the relative efficacy of $ZnPcS_4$-based PDT. One finding of our study was that after an administration of 2.0 mg/m^2 of $ZnPcS_4$ by the tail vein, the mild fluorescence in normal choriocapillaris and the maximal fluorescence in CNV was detected at 20 min. Therefore, PDT for choroidal vessels is most likely effective within 10–20 min after the administration of $ZnPcS_4$ at the 2.0 mg/m^2 dose. We cannot exclude the possibility of postmortem photosensitizer diffusion across tissue boundaries before fluorescence microscopy as a result of the cryostat sectioning techniques; however, in the case of fluorescein, this occurrence was believed to be unlikely. We cannot continuously observe photosensitizer uptake and clearance without videoangiography. For these reasons our protocol was based on the result presented by Haimovici and colleagues[18] and Kliman and coauthors.[19] Our study indicated that for the hydrophilic photosensitizer $ZnPcS_4$, the optimal time for laser irradiation following dye injection is between 10 and 20 min.

Experiments in monkeys and human clinical trials have shown an optimal irradiance of 600 mW/cm^2, and fluence of 50 J/cm^2 delivered over 83 s.[20,21] These parameters provide the maximal

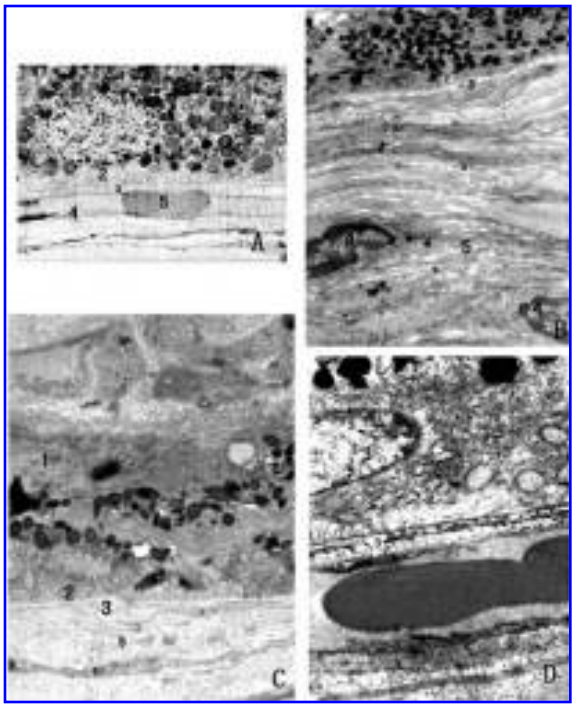

FIG. 5. Electron micrograph (**A–D**) taken pre- and postphotodynamic therapy (PDT). (**A**) Electron micrograph of normal rat retina. The nucleus of retinal pigment epithelium (RPE) (1) were clear with a lot of pigment granules, a double layer of plasma membrane infolding (2) above the basement membrane line up in order, Bruchi's membrane (3) is continuous in its integrity, the wall of surrounding choriocapillaris (4) were smooth with intact red blood cell (5) in it (×3600). (**B**) Electron micrograph of the edge of an untreated CNV lesion enveloped by proliferating RPE (1) along with plasma membrane infolding (2), and Bruch's membrane (3). The prominent endothelial cells (4) and massive collagen fibers (5) of treated CNV have lost normal cellular structure (×6000). (**C**) Electron micrograph of a capillary in an untreated CNV lesion, showing proliferating RPE cells (1) with plasma membrane infolding (2), active fibroblasts (3), endothelial cells (4), and massive collagen fibers (5) (×4800). (**D**) The choriocapillaris has no significant damage. Note also some swelling and destruction of the mitochondria in the RPE cells (1) at the site of the PDT. The plasma membrane infolding (2) and Bruch's membrane (3) is continuous in its integrity, the choriocapillaris (4) was smooth with an intact red blood cell (5) in it (×4800).

therapeutic effect of PDT while minimizing the collateral damage to surrounding normal structures. In our study, the angiographic closure of the CNV lesion in the rat model also showed a time dependency. Twenty-four (24) hours post-treatment, rats receiving $ZnPcS_4$ alone without PDT or laser irradiation alone without $ZnPcS_4$ did not show a significant closure rate. The 24-h closure rate in these rats was 25% and increased to 67% at the 7-day post-treatment. This result was different from the results obtained by David and coauthors,[15] who presented evidence that a detectable and dose-response curve was crucial to the testing of adjuvant therapies, because they could monitor for shifts in these response curves as a function of different pharmacologic agents. Successful adjuvants to PDT would cause an increase in the CNV closure rate at the lower drug dose and lower light-energy doses.

Our study validated the reliability of photosensitizer $ZnPcS_4$-based PDT with FFA and OCT combined with light and electric histopathology, which had not been performed in previous studies. PDT caused the destruction of the vascular channels and an organization of the CNV complex into a scar. OCT is a useful technique in describing morphologic findings of the retina and choroid.[22] In our study, OCT showed a double-layered structure in the normal sensory retina with a highly reflective layer, which was quite different from OCT findings in the human retina. The two reflective bands in the OCT images were identified as coming from the inner layers of the retina and from the photoreceptors. The highest reflective band arose from the RPE and choriocapillaris. Some high reflex areas corresponded with the CNV that consisted of newly formed blood vessels with wide vascular lumens and proliferated spindle-shaped RPE cells. Sahni and coworkers[23] presented a new terminology to validate the reliability of OCT and studied the effect of PDT in patients with subfoveal, predominantly classic CNV secondary to AMD.

Our study characterized only the short-term (7 days) vessel closure produced by $ZnPcS_4$–PDT. A longer follow-up of experimental animals would be required to assess the recurrence rate after the initially successful PDT of CNV. A limitation of the animal model of CNV is the spontaneous regression of neovascularization, even in the absence of any treatment. Therefore, much further work is needed before $ZnPcS_4$–PDT can be considered for use in human eyes. One limitation of the current PDT treatment regimen was in the damage to normal structures, thus potentially limiting the number of repeat treatments and drug and light doses that could be applied safely. $ZnPcS_4$–PDT would be demonstrated to have less damage to normal structure.

CONCLUSIONS

In conclusion, $ZnPcS_4$ was found to localize selectively in the choriocapillaris and CNV on fluorescence microscopy. $ZnPcS_4$–PDT is a potential new strategy for the treatment of macular degeneration and other human diseases manifesting as CNV. Many factors contribute to photodynamic effectiveness: concentration, fluence, wavelength, time to treatment, and localization within CNV. Whether the observed activation times are suitable for clinical applications remains to be determined. Further investigations are required to explore the optimal method for CNV occlusion, including refinement of $ZnPcS_4$ concentrations, light dosage parameters, and the necessity of retreatment.

ACKNOWLEDGMENTS

This study was funded, in part, by the National Natural Science Foundation of China (No. 20604007) and by the Fujian Provincial Science Foundation (No. C0510007). The authors thank Jianxin Wang and Jianshi Hu for their help with the observation of fluorescence microscopy.

REFERENCES

1. Holz, F.G., Jorzik, J., Schutt, F., et al. Agreement among ophthalmologists in evaluating fluorescein angiograms in patients with neovascular age-related macular degeneration for photodynamic therapy eligibility (FLAP-Study). *Ophthalmology* 110:400–405, 2003.
2. Reed, M.W.R., Miller, F.N., Wieman, T.J., et al. The effect of photodynamic therapy on the microcirculation. *J. Surg. Res*. 45:452–459, 1988.
3. He, D.P., Hampton, J.A., Keck, R., et al. Photodynamic therapy: Effect on the endothelial cell of the rat aorta. *Photochem. Photobiol*. 54:801–804, 1991.
4. Miller, H., and Miller, B. Photodynamic therapy of subretinal neovascularization in the monkey eye. *Arch. Ophthalmol*. 111:855–860, 1993.
5. Kliman, G., Puliafito, C., Stern, D., et al. Phthalocyanine photodynamic therapy: New strategy for closure of choroidal neovascularization. *Lasers Surg. Med*. 15:1–10, 1994.
6. The Verteporfin in Photodynamic Therapy Study Group. Verteporfin therapy of subfoveal choroidal neovascularization in age-related macular degeneration: Two-year results of a randomized, clinical trial including lesions with occult with no classic choroidal neovascularization—verteporfin in photodynamic therapy report 2. *Am. J. Ophthalmol*. 131:541–560, 2001.
7. Blumenkranz, M.S., Woodbum, K.W., Oing, F., et a1. Lutetium Texaphrin (Lu-Tex): A potential new agent for ocular fundus angiography and photodynamic therapy. *Am. J. Ophthalmol*. 129(3):353–362, 2000.
8. Mori, K., Yoneya, S., Anzail, K., et al. Photodynamic therapy of experimental choroidal neovascularization with a hydrophilic photosensitizer: Mono-L-aspartyl chlorin e6. *Retina* 21:499–508, 2001.
9. Peyman, G.A., Moshfeghi, D.M., Moshfeghi, A., et al. Photodynamic therapy for choriocapillaris using tin ethyl etiopurpurin (SnET2). *Ophthalmic Surg. Lasers* 28:409–417, 1997.
10. Takahashi, H., Itoh, Y., Miyauchi, Y., et al. Activation of two caspase cascades, caspase 8/3/6 and caspase 9/3/6, during photodynamic therapy using a novel photosensitizer, ATX-S10 (Na), in normal human keratinocytes. *Arch. Dermatol. Res*. 295:242–248, 2003.
11. Ciulla, T.A., Criswell, M.H., Snyder, W.J., et al. Photodynamic therapy with PhotoPoint photosensitiser MV6401, indium chloride methyl pyropheophorbide, achieves selective closure of rat corneal neovascularisation and rabbit choriocapillaris. *Br. J. Ophthalmol*. 89:113–119, 2005.
12. Kliman, G.H., Puliafito, C.A., Stern, D., et al. Phthalocyanine photodynamic therapy: New strategy for closure of choroidal neovascularization. *Lasers Surg. Med*. 15:2–10, 1994.
13. Haywood-Small, S.L., Vernon, D.I., Griffiths, J., et al. Phthalocyanine-mediated photodynamic therapy induces cell death and a G0/G1 cell cycle arrest in cervical cancer cells. *Biochem. Biophys. Res. Commun*. 339:569–576, 2006.
14. Dobi, E.T., Puliafito, C.A., Destro, M., et al. A new model of experimental choroidal neovascularization in the rat. *Arch. Ophthalmol*. 107:264–269,1989.
15. David, N., Zacks, E.E., Yoshiko, T., et al. Verteporfin photodynamic therapy in the rat model of choroidal neovascularization: Angiographic and histologic characterization. *Invest. Ophthalmol. Vis. Sci*. 43:2384–2391, 2002.
16. Peèkaitytëa A, Daugelavièiusa R, Sadauskaitëa A., et al. Comparative analysis of the photobactericidal action of selected tetrapyrrole compounds on Gram-positive and Gram-negative bacteria. *Biologija*. 11:41–46, 2005.
17. Borgatti-Jeffreys, A., Hooser, S.B., Margaret, A., et al. Preclinical evaluation of zinc phthalocyanine tetrasulfonate-based PDT. *Photon. Therapeut. Diagnost*. 5686:624–630, 2005.
18. Haimovici, R., Ciulla, T.A., Miller, J.W. et al. Localization of rose bengal, aluminum phthalocyanine tetrasulfonate, and chlorin e6 in the rabbit eye. *Retina* 22:65–74, 2002.
19. Kliman, G.H., Puliafito, C.A., Grossman, G.A. et al, Retinal and choroidal vessel closure using phthalocyanine photodynamic therapy. *Lasers Surg. Med*. 15:11–8, 1994.
20. Miller, J.W., Walsh, A.W., Kramer, M., et al. Photodynamic therapy of experimental choroidal neovascularization using lipoprotein-delivered benzophorphyrin. *Arch. Ophthalmol*. 113:810–818,1995.

21. Miller, J.W., Schmidt-Erfurth, U., Sickenberg, M., et al. Photodynamic therapy with verteporfin for choroidal neovascularization caused by age-related macular degeneration: Results of a single treatment in a phase 1 and 2 study. *Arch. Ophthalmol*. 117:1161–1173,1999
22. Rogers, A.H., Martidis, A., Greenberg, P.B., et al. Optical coherence tomography findings following photodynamic therapy of choroidal neovascularization. *Am. J. Ophthalmol*. 134:566–576, 2002.
23. Sahni, J., Stanga, P., Wong, D., et al. Optical coherence tomography in photodynamic therapy for subfoveal choroidal neovascularisation secondary to age-related macular degeneration: A cross-sectional study. *Br. J. Ophthalmol*. 89:316–320, 2005.

Received: November 11, 2006
Accepted: May 8, 2007

Reprint Requests:
Guoxing Xu
Department of Ophthalmology
Shadong University
Fuzhou
China

E-mail: zjfmuxgx@pub5.fz.fj.cn